EUROPEAN ORGANIZATION FOR NUCLEAR RESEARCH

HR/afm/is CERN/PS/AA/83-22

THE TRIGGERED PSEUDO-SPARK

J. Christiansen, K. Frank, H. Riege and R. Seeböck

Paper to be presented at the XVIth International Conference on Phenomena in Ionized Gases, Düsseldorf, August 29-September 2, 1983.

Geneva, Switzerland
April 1983

THE TRIGGERED PSEUDO-SPARK

J. Christiansen, K. Frank, H. Riege and R. Seeböck
CERN, Geneva, Switzerland
and Physikalisches Institut der Universität Erlangen - Nürnberg,
Erlangen, Fed. Rep. of Germany

Introduction

The pseudo-spark[1,2] is a low pressure gas discharge on the left branch of the Paschen curve. In its basic form it occurs between two plane electrodes with a centre hole (Fig. 1).

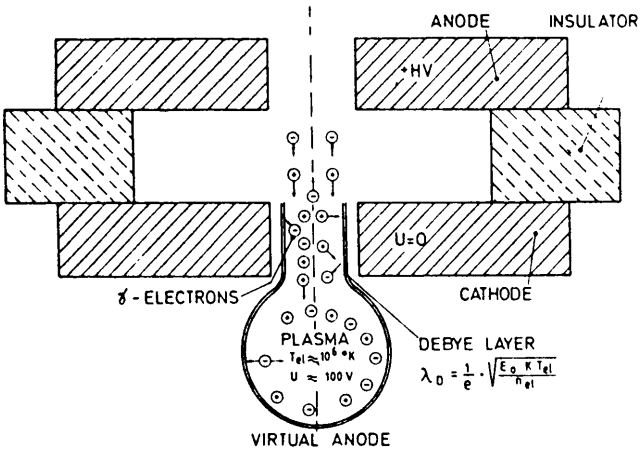

Fig. 1: Basic pseudo-spark configuration

When a voltage is applied to the gap, the equipotential planes form bumps through the holes. The effective distance for breakdown is then greater than the electrode spacing, and the discharge tends to start on the axis of the holes. Electrons created by ionization are immediately lost in the anode region, whereas the positive ions travel through the cathode hole and build up a virtual anode. The potential of this virtual anode is of the order of 100 V with respect to the cathode for a charging voltage of 20 kV. The virtual anode is enclosed by a Debye sheath, where the virtual anode potential gives rise to a high electric field, which eases the transport of ions to the cathode through the sheath. The γ-electrons produced by ion impact on the cathode surface enter the virtual anode just at their optimum ionization probability and, when oscillating inside the virtual anode, they rapidly increase the charge carrier density in this region. A fast breakdown occurs, accompanied by the formation of an intense electron beam directed towards the anode and an ion-beam leaving the virtual anode in the opposite direction. Total current densities far beyond the Langmuir-Child limit can be obtained. The ion current density limitation is now given by Bohm's equation:

where n_{el} is the electron density, T_{el} the electron temperature, m_i the ion mass, and A a factor close to 1. The potential and the electrode distance in the Langmuir-Child law are replaced by the virtual anode potential and the Debye-length $\lambda_D = (\varepsilon_o\, k\, T_{el}/n_{el} e^2)^{1/2}$. The high total and beam current densities and the rapid breakdown of the pseudo-spark are useful in applications such as gas switches and pulsed beam sources.

Trigger Methods

The breakdown of the basic pseudo-spark configuration (Fig. 1) can be very efficiently triggered in the virtual anode region. Here we describe three different trigger methods which have been developed for fast power switching and pulsed electron and ion beam sources.

a) Dielectric Surface Breakdown Trigger

An isolated trigger electrode is embedded in the cathode between two dielectric foils of 0.3 mm thickness (Fig. 2). An external 2 kV pulse produces a spark across the dielectric layers inside the cathode hole. The plasma being formed by this discharge acts like the virtual anode and leads to breakdown of the main gap with a delay of less than 3 ns and with a jitter of less than 1 ns.

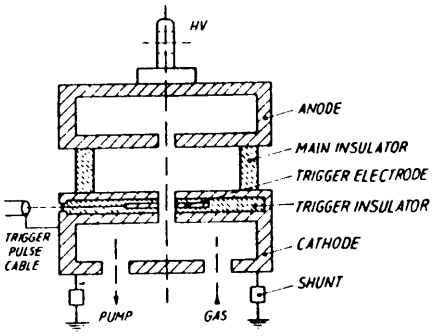

Fig. 2: Principle of the dielectric surface discharge trigger

The dielectric surface trigger can be separated and placed a few millimeters behind the cathode. Then delays of several tens of nanoseconds and 1 ns jitter are measured. The dielectric surface trigger is well suited for high voltage switches and multigap pseudo-spark chambers for beam generation. This trigger type is limited to medium power, since, even when placed outside the main gap, the dielectric surface may suffer.

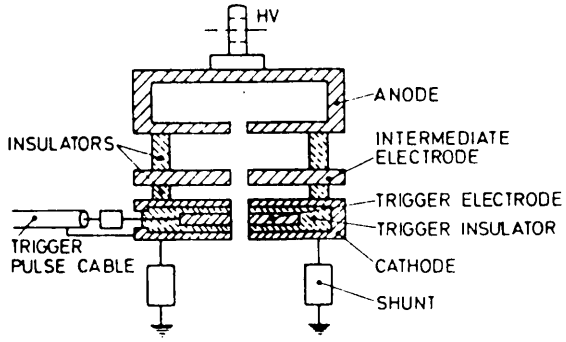

Fig. 3: Principle of the over-voltage trigger

b)Over-Voltage Trigger

The insertion of an intermediate electrode at floating potential into the main gap of a pseudo-spark chamber (Fig. 3) increases the breakdown voltage in a limited pressure range by a factor of up to 30. Fig. 4 shows three breakdown curves in helium of chambers, with and without an intermediate electrode.

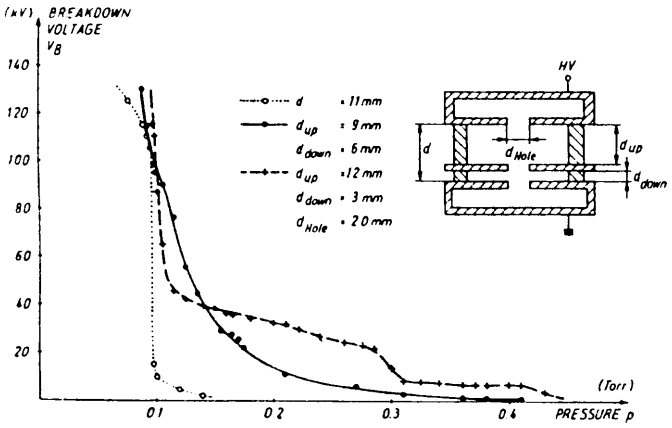

Fig. 4: Comparison of single-gap breakdown in helium with and without an intermediate electrode

The breakdown curves of those cases with intermediate electrodes are shifted to higher pressures. Higher breakdown voltages in the lower voltage and the higher pressure range are obtained with a large upper gap (d_{up} = 12 mm) and a small lower gap (d_{down} = 3 mm). In the case of rather equal upper and lower gap distances the behaviour in the higher voltage range is improved. These effects can be explained by charge collection on the intermediate electrode modifying the field distribution in the chamber, such that the field in the small gap is considerably enhanced but is reduced in the long gap. Short-circuiting of the small gap places the working poirt far above the breakdown curve of the long gap, and hence a strong over-voltage appears on the long gap, followed by rapid breakdown. The breakdown of the small gap (d_{down}) can be achieved with a dielectric surface breakdown trigger incorporated into the cathode (Fig. 3) as described above. Measured delay and jitter values are comparable to the pure surface trigger data. The over-voltage trigger is essentially suited for single-gap pseudo-spark switches up to 100 kV. They can be operated at higher pressure compared to switches without intermediate electrodes.

e) Electron Beam Trigger

A 1 mA, 2 keV electron beam is generated adjacent to the main pseudo-spark chamber in a d.c. discharge chamber with an inserted trigger electrode. The elecron beam travels through this electrode, the cathode, and the main gap of the switch. With the trigger electrode, the charge carrier multiplication in the virtual anode region is enhanced or suppressed by applying a negative or positive static potential of the order of 100 V (Fig. 5). A 40 kV main gap voltage has been switched by commutating the trigger electrode potential from +100 V to -200 V with a transistor. Switching delay and jitter were measured as a function of the hole diameter and the thickness of the trigger electrode, of its distance to the cathode, and of the charging voltage for a given total electron beam current and gas pressure. For a medium distance of 8 mm, a hole diameter of 2.5 mm and high voltages in the range from 5 to 10 kV, switching delays of 0.8 to 1.2 µs and jitter of 10 to 20 ns are obtained. This trigger type, which involves only metal electrodes but no dielectric surfaces, is predestined for high-current, high-power and multichannel-discharge type switches.

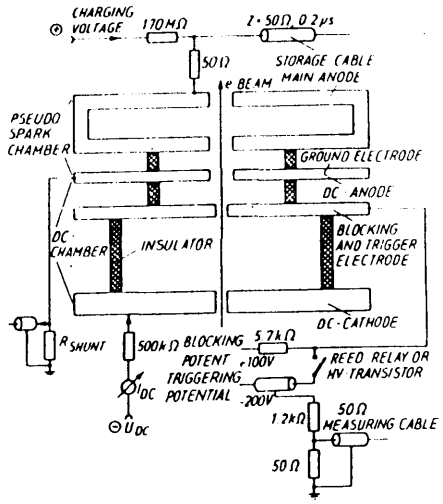

Fig. 5: Principle of the electron beam trigger

Conclusion

The breakdown mechanism in the pseudo-spark chambers allows very efficient triggering at the virtual anode. Appropriate trigger systems have been developed for application in high-voltage and/or high-current switching. The construction of cheap pseudo-spark switches as replacement for thyratrons, ignitrons, etc., as well as of cheap pulsed electron and ion beam sources seems to be possible.

References

1. J. Christiansen and C. Schultheiss, Z. Phys. A290, 35 (1979)

2. D. Bloess et al., Nucl. Instrum. and Methods 205, 173 (1983)

EUROPEAN ORCANIZATION FOR NUCLEAR RESEARCH

CERN/PS/BR/83-21
March 1983

A VARIABLE TRANSITION ENERGY LATTICE FOR SIS 12/18

B. Franczak, K. Blasche

GSI, Postfach 110 541, D-6100 Darmstadt 11, Germany

K.H. Reich

CERN, CH-1211 Geneva 23, Switzerland

Introduction and Summary

General

GSI plans to build a heavy ion synchrotron[1], SIS 12/18, as an extension to its UNILAC facility. This linear accelerator, in operation since 1976, accelerates heavy ions up to 20 MeV/u. SIS 12/18 will extend this range up to 1 GeV/u for the heaviest ions like uranium ($q/A \approx 0.3$), and even up to 2 GeV/u for light ions with a specific charge $q/A = 0.5$.

Acceleration of intense proton beams to 4.5 GeV ($\gamma = 5.8$) is being discussed as an option, for instance to produce exotic radionuclides, or for experiments comparing proton interactions with those of ions.

In normal operation a magnetic rigidity of 12 Tm can be reached in a fast cycle (dB/dt = 10 T/s, 3 cycles/s). For high energy operation up to 18 Tm, the power supplies are connected for giving a peak current of 3500 A at a reduced cycle rate (dB/dt = 4 T/s, 1 cycle/s).

Lattice

After comparative studies, a strictly periodic lattice with 12 identical cells was chosen for ion acceleration (Fig. 1). Its main advantages are reasonable aperture requirements and favorable ejection parameters, as well as sufficient working area in the Q_H-Q_V diagram for high intensity operation (see section 3). Depending on whether FODO, doublet or triplet quadrupole focusing is used, the machine parameter γ_t (see section 2) takes the following values:

Focusing	FODO	Doublet	Triplet
γ_t	3.8	5.4	4.2

While the γ-values of ions even at 2 GeV/u stay well below these γ_t values, acceleration of protons to $\gamma = 5.8$ would in all three cases mean crossing the transition energy. It is therefore proposed to modify in this case the lens currents for raising γ_t to, say $\gamma_t \approx 8$, while keeping the betatron tunes at $Q_H = 4.2$ and $Q_V = 3.4$ (section 2).

Presented at the
1983 Particle Accelerator Conference
Santa Fe, New Mexico

A VARIABLE TRANSITION ENERGY LATTICE FOR SIS 12/18

B. Franczak, K. Blasche
GSI, Postfach 11o 541, D-61oo Darmstadt 11, Germany

K.H. Reich
CERN, CH-1211 Geneva 23, Switzerland

Introduction and Summary

General

GSI plans to build a heavy ion synchrotron[1], SIS 12/18, as an extension to its UNILAC facility. This linear accelerator, in operation since 1976, accelerates heavy ions up to 2o MeV/u. SIS 12/18 will extend this range up to 1 GeV/u for the heaviest ions like uranium ($q/A \approx o.3$), and even up to 2 GeV/u for light ions with a specific charge $q/A = o.5$.

Acceleration of intense proton beams to 4.5 GeV ($\gamma = 5.8$) is being discussed as an option, for instance to produce exotic radionuclides, or for experiments comparing proton interactions with those of ions.

In normal operation a magnetic rigidity of 12 Tm can be reached in a fast cycle (dB/dt = 1o T/s, 3 cycles/s). For high energy operation up to 18 Tm, the power supplies are connected for giving a peak current of 35oo A at a reduced cycle rate (dB/dt = 4 T/s, 1 cycle/s).

Lattice

After comparative studies, a strictly periodic lattice with 12 identical cells was chosen for ion acceleration (Fig. 1). Its main advantages are reasonable aperture requirements and favorable ejection parameters, as well as sufficient working area in the Q_H-Q_V diagram for high intensity operation (see section 3). Depending on whether FODO, doublet or triplet quadrupole focusing is used, the machine parameter γ_t (see section 2) takes the following values:

Focusing	FODO	Doublet	Triplet
γ_t	3.8	5.4	4.2

While the γ-values of ions even at 2 GeV/u stay well below these γ_t values, acceleration of protons to $\gamma = 5.8$ would in all three cases mean crossing the transition energy. It is therefore proposed to modify in this case the lens currents for raising γ_t to, say $\gamma_t \approx 8$, while keeping the betatron tunes at $Q_H = 4.2$ and $Q_V = 3.4$ (section 2).

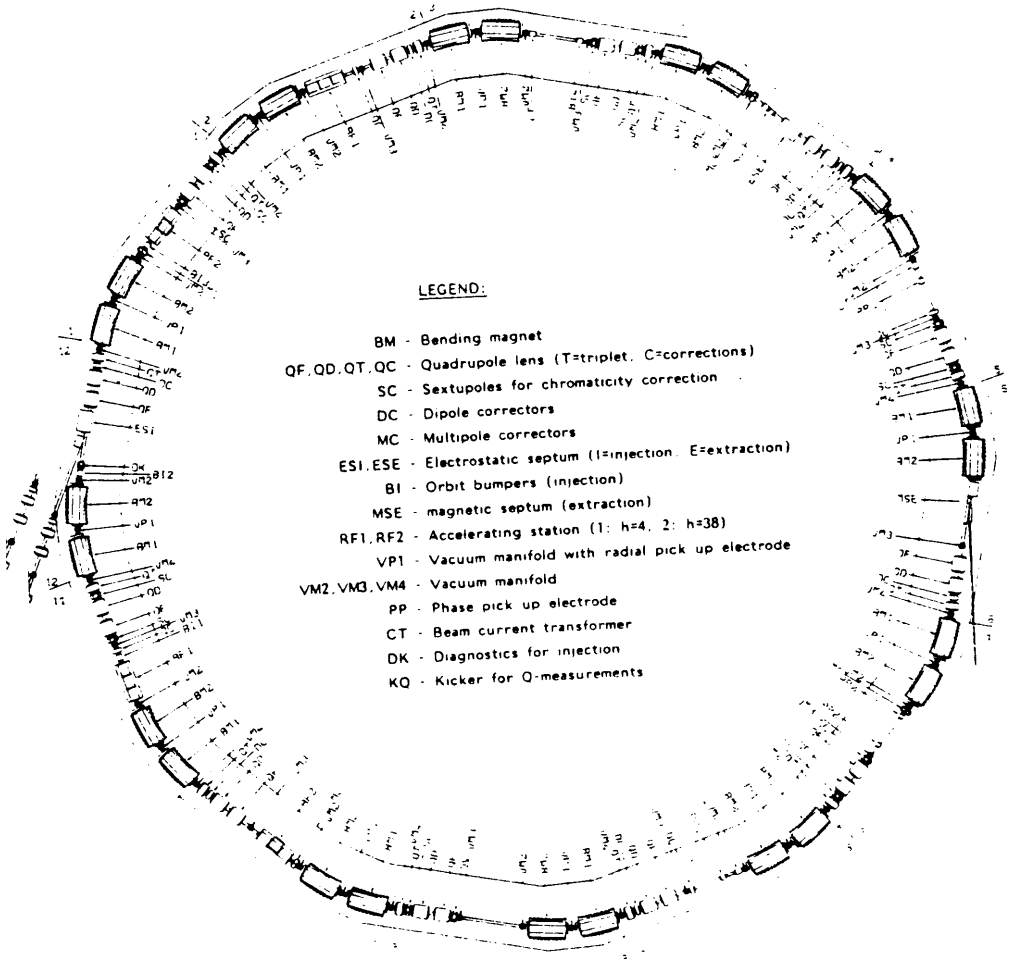

Fig. 1: Layout of Heavy Ion Synchrotron SIS 12/18. Use of triplet focusing at low energy increases machine acceptance. Modulation of doublet current (S = 6) raises transition energy when accelerating protons to 4.5 GeV.

Lattices with Variable Transition Energy

At transition energy the revolution time is, per definition, independent of particle momentum: the gain in time due to the higher velocity of a particle with a higher momentum $\delta p/p$ is cancelled by the extra time needed to complete its equilibrium orbit with added length δL. One has for the normalised energy, γ_t:

$$\gamma_t^2 = \frac{1}{\text{momentum compaction factor}} = \frac{\delta p/p}{\delta L/L} ; \qquad (1)$$

the RHS can be read as nominal orbit length divided by the added length of an equilibrium orbit with $\Delta p/p = 1$. The shorter this added length, the higher γ_t and vice versa.

The length difference δL is given by the off-momentum orbit $x_p(s)$ and the bending radius $\rho(s)$:

$$\delta L = \int_0^L [x_p(s)/\rho(s)]ds . \qquad (2)$$

Using the method of Fourier components for arriving at the off-momentum orbit[2], this becomes:

$$\delta L = 2\pi\, Q^3\, \delta p/p \sum_k a_k^2/(Q^2 - k^2) , \qquad (3)$$

where Q is the betatron tune and the coefficients a_k are given by:

$$a_k = (1/2\pi) \int_0^{2\pi} [\beta^{3/2}(\phi)/\rho(\phi)]e^{-ik\phi}d\phi$$

with β the amplitude function and $\phi = \int_0^L ds/(Q\bar{\beta})$.

Using (3), equation (1) becomes:

$$\gamma_t^2 = (2\pi\, Q^3/L) \sum |a_k^2|/(Q^2 - k^2) . \qquad (4)$$

One way to change γ_t is hence to introduce a superperiodicity, for example by arranging the bending magnets as shown in Fig. 2b.

The solution chosen here is to create the Fourier component wanted by means of differential excitation of the main quadrupoles. Firstly, this solution allows one to tune independently γ_t and Q_H, Q_V. Secondly, since the machine geometry is unchanged, γ_t tuning can be used only when really needed, i.e. for accelerating protons to higher energies in the present case.

For a small modulation of the amplitude function β by a term $(a/Q)\sin n\phi$ one has[3] with R = machine radius:

$$\gamma_t^2 \approx Q^2 - \frac{9}{8}\frac{Q^2}{R^2}\,\frac{Q^4}{Q^2 - n^2} . \qquad (4a)$$

From equ. (3) or (4a) the requirements are immediately clear: to raise γ_t one has to create a harmonic just above Q and to lower γ_t a harmonic below Q.

Fig. 2c shows the beam envelopes and the off-momentum orbit after modulating the lens strength (with a superperiodicity S = 6) to reach $\gamma_t \approx \infty$. While the vertical envelope does not change with γ_t (as designed), the horizontal amplitude function unavoidably increases locally. However, in practice, this should not cause a problem, as less lens strength modulation is required to reach $\gamma_t \approx 8$ and the modulation can be done later in the cycle, when the emittance has sufficiently shrunk. Fig. 2d shows that this scheme works also with a FODO

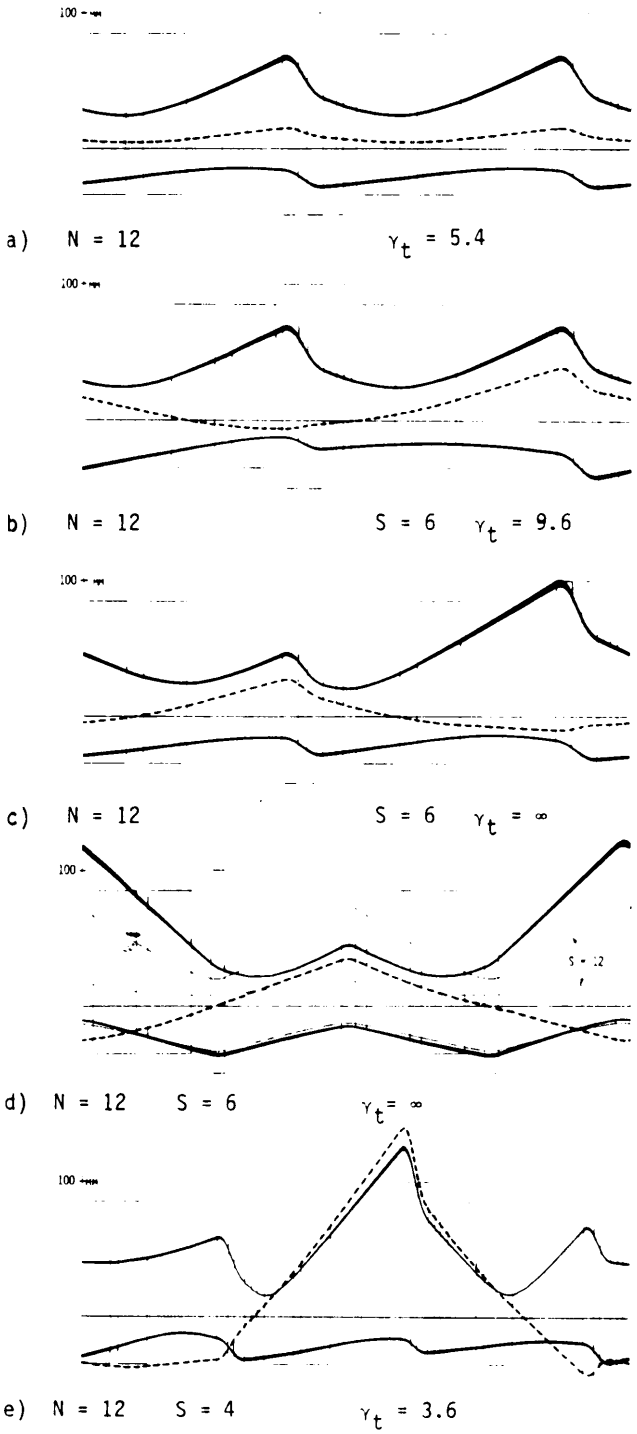

Fig. 2: Changing γ_t by introducing a superperiodicity. Horizontal (above) and vertical (below) beam envelopes $\sqrt{\beta\varepsilon}$, and off-momentum orbit x_p (---) are shown for: $\varepsilon_H = 16\pi$, $\varepsilon_V = 4\pi$ mm mrad, $\delta p/p = \pm$ 0.5 %, $Q_H = 4.2$, $Q_V = 3.4$ (Doublet focusing, except d).
a) Strictly periodic lattice; $\gamma_t = 5.4$.
b) Bending magnets arranged with S = 6; $\gamma_t = 9.6$.
c) Quadrupoles excited with S = 6; $\gamma_t \approx \infty$
d) Idem c) but for FODO focusing.
e) Quadrupole excited with S = 4; $\gamma_t = 3.6$.

lattice, the envelope variation being somewhat larger though. Note that because of these large changes equ. (4) rather than (4a) has to be used.

For academic interest, a case of lowering γ_t is shown in Fig. 2e. Using S = 4, γ_t = 3.6 was reached, though necessarily at the expense of large local increases in β_H and x_p. More refined methods[4] should presumably be used to obtain such a reduction of γ_t with reasonable local increases of β_H and x_p.

The SIS 12/18 Lattice

The layout is shown in Fig. 1 and the beam envelopes in Fig. 2a. N = 12 was chosen as a reasonable compromise. A larger number of periods leads to smaller apertures but more elements and shorter straight sections, whereas a smaller number leads to longer straight sections and a lesser number of elements, but to bulkier bending magnets and larger apertures. The main reason for the strict periodicity (no superperiods) was the wish for sufficient working room free from systematic resonances up to 5th order in the Q_H-Q_V diagram (see Fig. 3). The tune difference ΔQ = 1 should minimise coupling. $Q_H > Q_V$ and an FD (rather than DF) doublet were adopted to achieve a high γ_t.

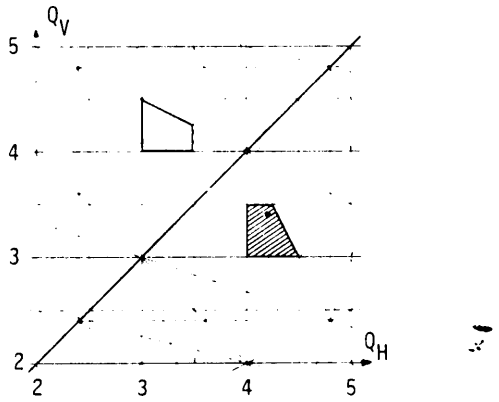

Fig. 3: Systematic (structural) resonances up to 5th order for N = 12. The hatched area is the preferred working area, but the symmetrically located area could also be used.

Because of the low injection energy of 1o MeV/u and the relatively weak ion currents (∿ 1oo μA) fairly large acceptances are required. Use of triplet focusing leads to net machine acceptances of A_H = 2oo and A_V = 5oπ mm mrad for full bending magnet apertures of 17o x 7o mm. Above 9 Tm (7oo MeV/u for q/A = o.5), doublet focusing is used with its lesser strength requirements, and easier beam extraction and chromaticity correction. Fig. 4 illustrates the dynamic change-over from triplet to doublet focusing. Calculations have shown that it should not be difficult to keep the tunes to o.o1 of their nominal values during this operation, using relatively simple power supply voltage programs.

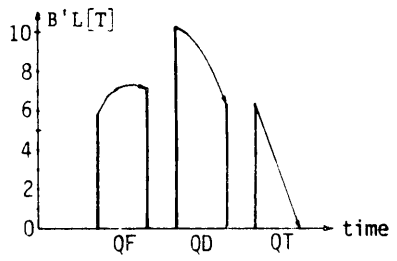

Fig. 4: Variation of quadrupole strength B'L during dynamic change-over from triplet to doublet focusing for constant values Q_H = 4.2, Q_V = 3.4

Fig. 5 shows the change-over to S = 6 for reaching $\gamma_t \approx \infty$ (Fig. 2c). As Q_V = 3.4, the potential systematic stopband 2 Q_V = 6 should be kept as narrow as possible.

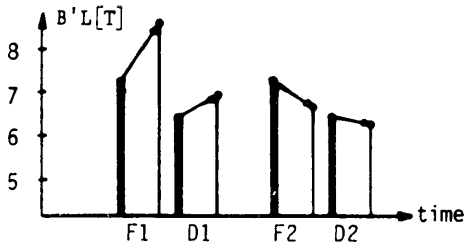

Fig. 5: Quadrupole strengths B'L of the four lens sets during the change-over to S = 6 and $\gamma_t \approx \infty$

This is done by using the remaining free parameter (4 lens strengths available to adjust γ_t, Q_H, Q_V) to minimise κ, the excitation coefficient[5]:

$$\kappa = \frac{SR}{8\pi B\rho} \int_0^{2\pi/S} \beta_V(\theta) B'(\theta) e^{i(2\mu_V - \theta\varepsilon)} d\theta \qquad (5)$$

where B' = field gradient, μ_V = betatron phase advance, θ = s/R, and $\varepsilon = 2Q_V - S$. For the present case equ. (5) has to be expressed in terms of the four quadrupole strengths, i.e. the summation must be made separately for each cell of the superperiod. Fig. 6 shows the value of κ as a function of B' in the quadrupole F1 of Fig. 5. The situation shown in Fig. 2c corresponds to the minimum value of κ. Under these conditions this stopband should not be detrimental, even at high intensities and the corresponding substantial space-charge tune shifts. The same optimisation leads to practically unchanged β_V-values.

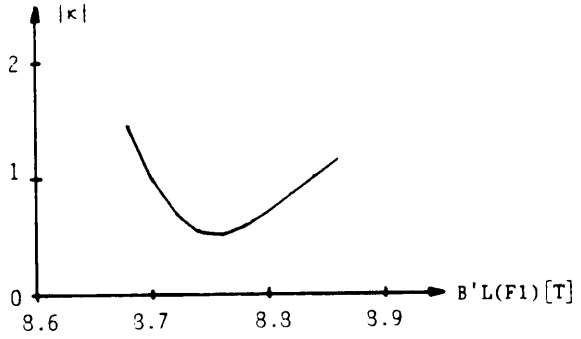

Fig. 6: Value of excitation coefficient κ as a function of strength B' of quadrupole F1 (Fig. 5)

References:

1. SIS, Eine Beschleunigeranlage für Schwere Ionen Hoher Energie, GSI 82-2, 1982
2. E.D. Courant, H.S. Snyder, Theory of the Alternating-Gradient Synchrotron, Annals of Phys., Vol. 3, 1958, p. 42.
3. L.C. Teng, Compensation of Space-Charge Mismatch at Transition of Booster Using the Transition-Jump Method, NAL FN-2o7, 197o
4. W. Hardt, A Large Change of γ_t, CERN MPS/DL 7o-16 197o, and Proc. X Int. Acc. Conf. 1974, p. 434.
5. G. Guignard, A General Treatment of Resonances in Accelerators, CERN 78-11, 1978, p. 48